Journal of Catalysis 460 (2026) 116896

Contents lists available at ScienceDirect

Journal of Catalysis

journal homepage: www.elsevier.com/locate/jcat

Research article

Carbon dioxide hydrogenation to formate catalyzed by phosphine-free ruthenium(0) cyclopentadienone complexes stabilized by NHC ligands

Sylwia Kostera [a,1], Chiara Lenzi [b,1], Saikat Pal [a], Francesco Calcagno [b,c], Ivan Rivalta [b,c], Rita Mazzoni [b,c,*], Luca Gonsalvi [a,*]

[a] Consiglio Nazionale delle Ricerche (CNR), Istituto di Chimica dei Composti Organometallici (ICCOM), Via Madonna del Piano 10, 50019 Sesto Fiorentino (Florence), Italy
[b] Dipartimento di Chimica Industriale "Toso Montanari", Università degli Studi di Bologna, Plesso Navile Ue4, Via Gobetti 85, 40129 Bologna, Italy
[c] Center for Chemical Catalysis – C^3, University of Bologna, Via Gobetti 85, 40129 Bologna, Italy

ARTICLE INFO

Keywords:
Carbon dioxide hydrogenation
Ruthenium
N-heterocyclic carbenes
Homogenous catalysis
Mechanistic studies

ABSTRACT

Phosphine-free ruthenium complexes containing a strongly donating 1,3-dimethyl-imidazolyl NHC ligand were tested for homogeneous catalytic CO_2 hydrogenation to formate under various reaction conditions, both with and without the addition of trimethylamine *N*-oxide (TMANO) as a co-catalyst. Under optimized conditions (80 bar, 100 °C), using *N*-methylpyrrolidone (NMP) as solvent and in the presence of TMANO, turnover numbers (TONs) exceeding 54,000 were achieved in single batch runs. Mechanistic studies by NMR spectroscopy and DFT calculations elucidate key steps and energies associated with the reaction pathway for the best performing catalyst, leading to a proposed mechanism.

1. Introduction

CO_2 hydrogenation is a chemical process in which carbon dioxide (CO_2) is converted into a series of C1 products, ranging from formic acid (HCOOH), formaldehyde (HCHO), methanol (CH_3OH), methane (CH_4) and hydrocarbons by reaction with hydrogen (H_2) under pressure. This process is of significant interest in the context of sustainable chemistry and carbon capture and utilization (CCU) strategies, as it offers a way to use a greenhouse gas to produce valuable chemicals and fuels [1], contributing to circular economy while addressing the challenges of climate change [2]. Due to the high thermodynamic stability of CO_2, these processes need to be carried out in the presence of suitable, active catalysts, whose design plays a crucial role in this process, as they enhance reaction rates and selectivity toward the desired products for a wide range of applications [3].

Homogeneous CO_2 hydrogenation to produce formic acid (HCOOH) has been effectively accomplished using a range of transition metals combined with diverse ligand frameworks. The most significant advancements, typically measured by metrics such as turnover numbers (TONs) and turnover frequencies (TOF, h^{-1}), currently define the state-of-the-art for this process. The most active catalysts predominantly involve platinum group metals (PGMs) such as ruthenium (Ru), rhodium (Rh) and iridium (Ir), stabilized by ligands including organophosphines, bipyridines, cyclic diimines, and pincer-type PNP ligands. In 2014, Pidko and co-workers established the state-of-the-art for Ru-catalyzed CO_2 hydrogenation to formate with the pincer-type complex [RuH(Cl)(CO)(PNP-^{t}Bu)] as catalyst [PNP-^{t}Bu = 2,6-Bis(di-*tert*-butylphosphinomethyl)pyridine], reaching TON = 200,000 and TOF = 1,100,000 h^{-1} in the presence of 1,5-diazabicyclo(5.4.0)undec-7-ene (DBU) as base, *N,N*-dimethylformamide (DMF) as solvent, 60 bar H_2/CO_2 (3:1) and 120 °C [4]. Previously, Nozaki and coworkers demonstrated the efficient use of the isopropyl-substituted PNP-pincer iridium tris(hydride) complex [Ir(H)$_3$(PNP)] [PNP = 2,6-bis((diisopropylphosphino)methyl)pyridine] as a catalyst for this process. Potassium formate was obtained with TONs up to 3,500,000 and TOFs of 150,000 h^{-1}, in the presence of KOH, tetrahydrofuran (THF) as solvent, 50 bar H_2/CO_2 (1:1), 200 °C [5]. More recently, precious metal-like performances were demonstrated using Earth-abundant metal-based homogeneous catalysts of Ni(II), Fe(II) and

Abbreviations: CCU, Carbon Capture and Utilization; TON, turnover number; TOF, Turnover Frequency; THF, tetrahydrofuran; NMP, *N*-methylpyrrolidone; TMANO, trimethylamine-*N*-oxide; TMA, trimethylamine.

* Corresponding authors.
E-mail addresses: rita.mazzoni@unibo.it (R. Mazzoni), l.gonsalvi@iccom.cnr.it (L. Gonsalvi).
[1] These authors equally contributed to this work.

https://doi.org/10.1016/j.jcat.2026.116896
Received 25 February 2026; Received in revised form 13 April 2026; Accepted 15 April 2026
Available online 24 April 2026

Mn(I) stabilized either by tetradentate NP_3 (for Ni) or tridentate pincer PNP ligands (for Fe and Mn) with TONs as high as 4,650,000, 60,000 and 2,000,000, respectively [6]. These developments have been comprehensively reviewed in the literature [3c–3f,7]. In recent years, many research groups have focused on the use of pincer-type ligands containing phosphorus donor atoms, that have the advantage of being easily synthetically tuned, and can confer remarkable stability to the metal center due to their tridentate nature, binding exclusively in meridional coordination mode [8]. As phosphorus is nowadays considered an endangered element, the design of active, phosphorus-free ligands and complexes is highly desirable.

At present, few examples of stable phosphorus-free, non-pincer-type complexes with easily dissociable ancillary ligands (e.g. CH_3CN, Cl, Br) that allow gaseous substrates activation, have been used as catalysts for homogeneous CO_2 hydrogenation and are summarized in Fig. 1. The well-known Knölker's hydrogenation catalyst (**Fe1**) and a library of efficient, stable, phosphine-free, and easy-to-synthesize derivatives of type $[Fe(CO)_3(L)]$ (L = substituted diaminocyclopentadienone), were developed for CO_2 hydrogenation [9]. CO_2 hydrogenation in the presence of Knölker's complex was reported by Yang, Zhou, and coworkers. In the first step NaOH (3 mmol) was converted to sodium bicarbonate in the presence of CO_2 (20 bar), then the Fe catalyst (0.003 mmol) was added to the solution and pressurized to 30 bar of hydrogen. Formate was obtained in 31% yield after 24 h, reaching a maximum TON of 307 [10]. Poater, Renaud, and coworkers described modification of Knölker's complex through subtle variations of the substituents on the aminocyclopentadienone ring (Fig. 1) [11]. Quantitative yields of formate and TONs up to 3343 were obtained with the complex bearing a *N*-aminoethylenemorpholine substituted ring (**Fe2**) after 20 h using triethanolamine (TEOA) as base, water as a solvent, 60 bar H_2/CO_2 (2/1) total pressure, 100 °C. Interestingly, the authors showed that pre-catalyst activation was needed, and this was obtained by the addition of trimethylamine *N*-oxide (TMANO, 0.001 mmol, 0.02 mol%) to promote CO ligand dissociation freeing a coordination site on the metal. Under the same reaction conditions, a cationic water-soluble derivative of the Knölker's complex (**Fe3**) and its neutral analogue (**Fe4**) gave lower TONs of 875 and 97, respectively [11].

Among P-free ruthenium complexes (Fig. 2), Lv, Zhu, He, and coworkers demonstrated the capability of Shvo's catalyst for the hydrogenation of CO_2 to HCOOH [12]. Shvo's catalyst complex (**II** in the rest of the study) is a metal–ligand cooperative (MLC) complex that, upon activation, generates a monomeric Ru–H species that is an extremely active hydrogenation catalyst [13]. It features both an acidic proton on the tetracyclopentadiene (CPD) ligand and a loosely bound carbonyl group on the ruthenium atom. The authors showed that in the presence of Shvo's catalyst (0.025 mmol), H_2/CO_2 (1/1) 60 bar total pressure, *N*-methypyrrolidone (NMP) as solvent, 60 °C, 10 h, low TON = 4 was obtained. In the same study, it was shown that by adding LiCl as co-catalyst, CO_2 hydrogenation to CO, rather than the kinetically favorable formation of HCOOH, was achieved under mild conditions [12].

In the choice of suitable ancillary ligands to further improve Shvo-type complexes thermal stability and activity in catalysis, *N*-heterocyclic carbenes (NHC), known for their strong σ-donating properties, can be of interest as they increase the electron density at the metal atom and promote effective hydride transfer during hydrogenation and dehydrogenation processes. Furthermore, the covalent bonds between NHCs and metals are typically very strong, resulting in complexes that are structurally stable and resistant to the harsh reaction conditions often required for CO_2 hydrogenation [14]. For example, in 2010 Peris and coworkers demonstrated the use of bis(NHC) arene Ru complexes (Fig. 1, **Ru1**) in the reduction of carbon dioxide to formate, obtaining a rewarding TON = 23,000 with KOH, H_2O, 40 bar H_2/CO_2 (1/1), 200 °C, 75 h. The authors concluded that the high thermal stability of the complexes under reaction conditions was crucial to obtain high catalytic performances [15].

Some of us described the synthesis of Shvo's complex derivatives bearing different substituents on the cyclopentadienone ring and NHC ancillary ligands [16] and its compelling catalytic activity in hydrogen-borrowing reactions [17]. For the reasons described above, we thus investigated the activity of ruthenium-NHC complexes in catalytic hydrogenation of CO_2. Namely, in this study we present results on the use of a small library of phosphine-free ruthenium(0) complexes containing the strongly donating 1,3-dimethylimidazolyl ligand (Fig. 2, complexes **I** and **IV**) and their NHC-free precursors (Fig. 2, complexes **II, III** and **V**) as catalysts for the selective hydrogenation of CO_2 to formate in the presence of 1,8-diazabicycloundec-7-ene DBU as base. Additionally, two iron analogue complexes (Fig. 2, complexes **VI** and **VII**) were tested under the reaction conditions used with Ru complexes. The results of the catalytic tests, including the screening of complexes (**I–VII**), the reaction conditions and the study of the effect of TMANO as co-catalyst, are presented herein together with mechanistic details obtained by combined experimental (NMR) and computational (DFT) approaches for the best performing catalyst.

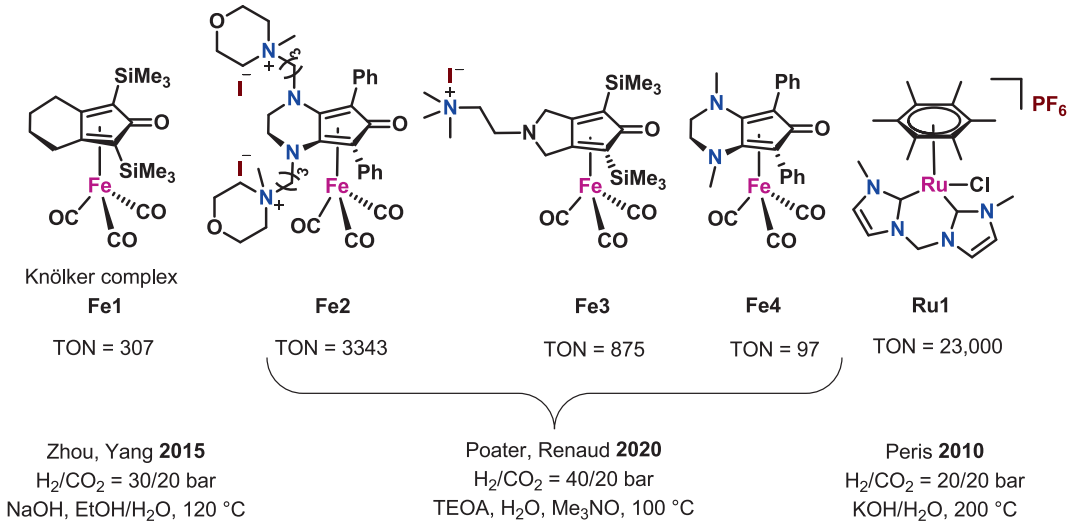

Fig. 1. Examples of P-free complexes tested as catalysts for CO_2 hydrogenation.

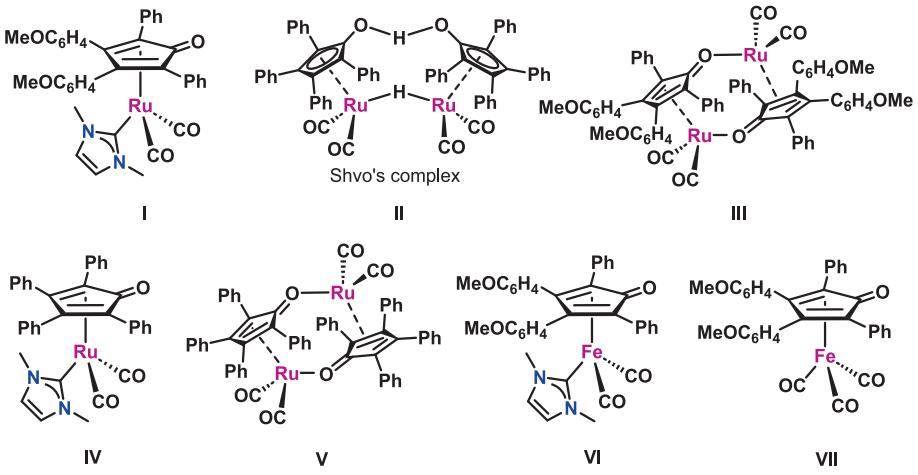

Fig. 2. Phosphine-free complexes tested in this study.

2. Results and discussion

2.1. Catalytic tests

Complex $[(\eta^4\text{-}PhOMe_2Ph_2C_4CO)(CO)_2Ru]_2$ (**III**) was synthesized from $Ru_3(CO)_{12}$ and 3,4-bis(4-methoxyphenyl)-2,5-diphenylcyclopenta-2,4-dienone [16], whereas **V** was obtained from of the reaction of $Ru_3(CO)_{12}$ and tetracyclone [17], both according to previously described methods. Complexes **III** and **V** served as precursors for the previously described Ru(NHC) complexes **I** and **IV**, which were obtained through a two-step synthetic method. Step 1 involved obtaining the appropriate silver complex from 1,3-dimethylimidazolium iodide and Ag_2O, and in step 2, the corresponding ruthenium dimer was added to produce complexes **I** [16] and **IV** (see Experimental Section). Shvo and coworkers reported the reaction of tetraphenylcyclopentadienone with $Ru_3(CO)_{12}$, resulting in the mono-metallic tris-carbonyl derivative $[Ru(Ph_4C_4CO)(CO)_3]$. Subsequent reaction of this tris(carbonyl) complex in a hydrogen donor solvent (e.g. methanol), affords Shvo's catalyst shown in Fig. 2 [13b,18]. Iron complexes **VI** and **VII** have been prepared following literature procedures [19]. CO_2 hydrogenation tests (Scheme 1) were initially carried out in the presence of **I** under previously reported conditions [20], i.e. using DBU as the base (1000 equiv.), H_2/CO_2 (1/1) 60 bar total pressure, 80 °C, 24 h.

In the initial screening of reaction parameters, the choice of the optimal solvent was evaluated. Using dry THF as the solvent and a DBU to catalyst ratio of 1/1000, formate was obtained with a yield of 50% (Table 1, entry 1) relative to DBU, resulting in a corresponding TON = 503. Addition of water to THF (1/10) caused a significant decrease in activity, yielding only 8% of formate (Table 1, entry 3). The use of NMP, a solvent of choice for other catalytic processes involving Shvo's complex-type catalysts [12], gave higher activity (Table 1, entry 2, yield 84%, TON = 847) and was thus selected for the remainder of the study. The influence of temperature on the reaction was then examined. Increasing the temperature from 80 °C to 100 °C led to an improvement in reaction efficiency. At a DBU to catalyst ratio of 1/2000, TON increased to 2010, with a substantial increase in yield to ≥ 99% (Table 1, entry 4). Conversely, a ratio of 1/5000 resulted in TON = 4486 (Table 1, entry 5). When the **I**/DBU ratio was changed to 1/10,000, formate was obtained with a yield of 43% and TON = 4314 (Table 1, entry 6). Changing the base from DBU to NEt_3 and increasing the temperature from 100 °C to 120 °C resulted in lower TON values (Table 1, entries 7

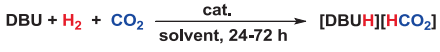

Scheme 1. General scheme and standard conditions for CO_2 hydrogenation tests in the presence of catalysts **I-VII** and DBU.

Table 1
Selected catalytic results for CO_2 hydrogenation to formate in the presence of catalyst **I**.

Entry	cat/DBU	Solvent	pH_2/pCO_2 (bar)	Temp. [°C]	TON [a]	Yield [b] (%)
1	1/1000	THF	30/30	80	503	50
2	1/1000	NMP	30/30	80	847	84
3	1/1000	THF/H_2O	30/30	80	84	8
4	1/2000	NMP	30/30	100	2010	≥99
5	1/5000	NMP	30/30	100	4486	89
6	1/10000	NMP	30/30	100	4314	43
7 [c]	1/10000	NMP	30/30	100	338	3
8	1/10000	NMP	30/30	120	3534	35
9	1/10000	NMP	40/40	100	5091	51
10	1/10000	NMP	60/20	100	6796	68

Reaction conditions: catalyst **I**, 1–10 μmol; DBU, 10 mmol; Solvent, 5.5 mL; 24 h. [a]TON = (mmol formate)/(mmol catalyst). [b]Yield = [(mmol formate)/(mmol DBU)] x 100. The amount of formate was calculated from the integration of the corresponding ^{1}H NMR signal in D_2O against an internal standard (DMF). [c]NEt_3 as a base. All experiments were repeated at least twice to check for reproducibility, average error ca. 6%.

Table 2
Selected catalytic results for CO_2 hydrogenation to formate in the presence of catalyst **I** and TMANO.

Entry	cat/DBU	cat/TMANO [c]	pH_2/pCO_2 (bar)	TON [a]	Yield [b] (%)
1	1/10000	–	40/40	5091	51
2	1/10000	–	60/20	6796	68
3	1/10000	1/100 [d]	30/30	9428	94
4	1/10000	1/100	60/20	10,052	≥99
5	1/20000	1/100	60/20	14,446	72
6	1/20000	1/50	60/20	11,211	56
7	1/20000	1/12.5	60/20	9493	47
8 [e]	1/20000	1/100	60/20	20,104	≥99
9	1/50000	1/100	60/20	15,451	31
10	1/50000	1/25	60/20	10,073	21
11 [e]	1/50000	1/100	60/20	46,698	93
12 [e]	1/50000	1/25	60/20	18,702	37
13 [e]	1/100000	1/100	60/20	54,442	54
14 [e]	1/200000	1/100	60/20	33,319	17

Reaction conditions: catalyst **I**, 0.05–1 μmol; DBU, 10 mmol; TMANO, 5–100 μmol; NMP, 5.5 mL; 100 °C; 24 h. [a]TON = (mmol formate)/(mmol catalyst). [b]Yield = [(mmol formate)/(mmol DBU)] x 100. The amount of formate was calculated from the integration of the corresponding ^{1}H NMR signal in D_2O against an internal standard (DMF). [c] TMANO in EtOH. [d]solid. [e]72 h. All experiments were repeated at least twice to check for reproducibility, average error ca. 6%.

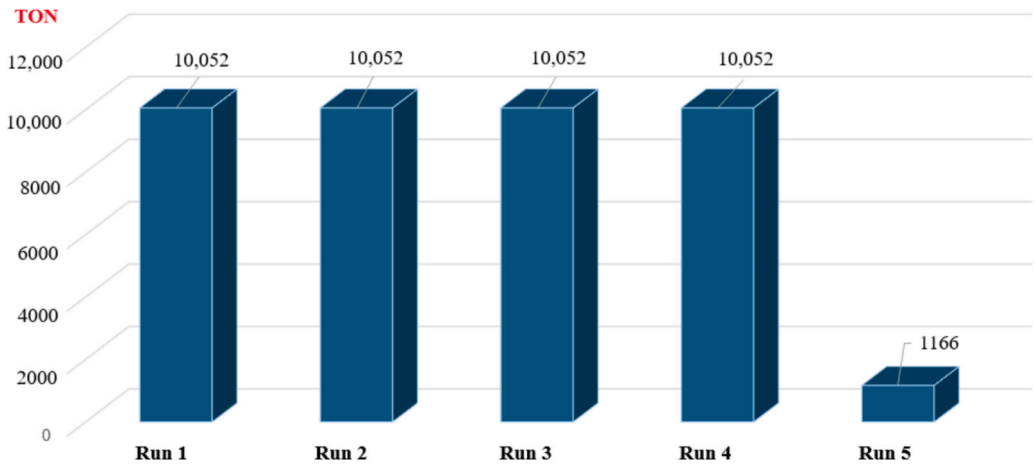

Fig. 3. TONs for catalyst recycling experiment using **I** under optimized conditions (cat/DBU = 1/10,000, cat/TMANO = 1/100, CO_2/H_2 = 1/3, 80 bar total pressure, NMP, 100 °C, 24 h).

Table 3
Selected catalytic results for CO_2 hydrogenation to formate in the presence of complexes **I-VII**.

Entry	Complex	cat/DBU	cat/TMANO [c]	pH_2/pCO_2 (bar)	TON [a]	Yield [b] (%)
1	**I**	1/5000	–	30/30	4486	89
2	**I**	1/10000	1/100	60/20	10,052	≥99
3	**II**	1/5000	–	30/30	5654	57
4	**II**	1/10000	1/100	60/20	1721	8
5	**III**	1/5000	–	30/30	3653	73
6	**III**	1/10000	1/100	60/20	4563	45
7	**IV**	1/5000	–	30/30	5026	≥99
8	**IV**	1/10000	1/100	60/20	10,052	≥99
9[d]	**IV**	1/100000	1/100	60/20	56,582	56
10	**V**	1/5000	–	30/30	3291	66
11	**V**	1/10000	1/100	60/20	2226	22
12	**VI**	1/5000	–	30/30	154	3
13	**VI**	1/10000	1/100	60/20	125	1
14	**VII**	1/5000	–	30/30	39	≥1
15	**VII**	1/10000	1/100	60/20	52	≥1

Reaction conditions: catalyst, 1–2 μmol; DBU, 10 mmol; TMANO, 0.1–0.2 mmol; NMP, 5.5 mL; 100 °C; 24 h. [a]TON = (mmol formate)/(mmol catalyst). [b]Yield = [(mmol formate)/(mmol DBU)] x 100. The amount of formate was calculated from the integration of the corresponding ^{1}H NMR signal in D_2O against an internal standard (DMF). [c] TMANO in EtOH. [d]72 h. All experiments were repeated at least twice to check for reproducibility, average error ca. 6%.

and 8, respectively). Next, the effect of increasing the gas mixture total pressure from 60 to 80 bar was tested, which led to a slight improvement in TON, increasing from 4314 to 5091 (Table 1, entry 9). The partial pressure ratio between H_2 and CO_2 was then modified from 30/30 to 60/20, resulting in a formate yield of 68% (Table 1, entry 10).

Next, the effect of trimethylamine *N*-oxide (TMANO) was tested. TMANO is a well-known CO scavenger in organometallic synthesis that works as an oxygen transfer reagent capable of converting coordinated carbon monoxide (CO) to labile CO_2 [21]. In catalytic runs with TMANO, an increase in activity was observed compared to the corresponding additive-free runs (Table 2, entries 1–4) [22]. However, due to the poor solubility of TMANO in NMP, it was decided to dissolve the desired amount in a minimum amount of ethanol and add the resulting solution to the catalytic mixture before starting the runs. In this way, TON values from 9428 to 10,052 (Table 2, entries 3 and 4, respectively) could be obtained. The effects of various TMANO to catalyst ratios on the reaction efficiency were then examined, using a DBU to catalyst ratio of 1/2000. Among the Ru/TMANO tested ratios of 1/100, 1/50 and 1/12.5 (Table 2, entries 5–7), the best results were observed with the ratios of 1/100 (Table 2, entry 5). Increasing the reaction time from 24 to 72 h, using a **I**/DBU ratio of 1/20,000 and a **I** to TMANO ratio of 1/100, resulted in a yield of ≥ 99% in formate (Table 2, entry 8). A DBU to catalyst ratio of 1/50,000 yielded formate with a maximum TON of 15,451 and a yield of 31% (Table 2, entry 9) in the presence of 0.02 mmol of TMANO (1/100), whereas a lower yield of 21% (TON = 10,073, Table 2, entry 10) was recorded with TMAO (1/25). The latter runs were repeated changing only the experiment duration (72 h), observing a significant increase in TON to 46,698 and 18,702, respectively (Table 2, entries 11 and 12). In addition, tests were performed using **I**/DBU ratios of 1/100,000 and 1/200,000, respectively. The reactions were carried out for 72 h, yielding TON values of 54,442 and 33,319 (Table 2, entries 13 and 14).

Proof-of-concept experiments were then run to evaluate catalyst recyclability, using the conditions applied for entry 4 in Table 2 (i. e. **I**/DBU = 1/10,000, **I**/TMANO = 1/100, CO_2/H_2 = 1/3, 80 bar total pressure, NMP, 100 °C, 24 h). After the first run, giving > 99% formate yield for a TON of 10,052, the autoclave was cooled to 10 °C, then the gas pressure was carefully released and replaced by nitrogen. A new aliquot of DBU (100% of the amount used in run 1) was added through the inlet port, without opening the autoclave, that was then re-pressurized with 80 bar CO_2/H_2 (1/3) and heated to 100 °C for 24 h (run 2). At the end of the reaction, formate was obtained in ≥ 99% yield (TON = 10,052). The two following runs were carried out as for run 2, giving the same results in yields and TONs. The fifth run yielded only 12% of formate (TON = 1166). Consequently, an overall TON = 41,374 was obtained after five consecutive runs under these conditions (Fig. 3). These experiments clearly demonstrate the possibility to efficiently recycle catalyst **I** for at least 4 consecutive runs at low catalyst loadings,

in the presence of TMANO as co-catalyst.

Next, the effect of substituent group variations on the cyclopentadienone ring was tested. Shvo's bimetallic catalyst **II** and the dimeric precursor of **I** (i. e. complex **III**) were tested for comparison with **I** (Table 3, entries 3–6). The yields of formate (57% with **II**, entry 3; 73% with **III**, entry 5, respectively) were lower compared to 89% obtained with **I** (Table 3, entry 1) in the absence of TMANO at a cat/DBU ratio of 1/5000. In the presence of TMANO at a cat/DBU ratio of 1/10,000, the yields were 8% and 45%, (Table 3, entries 2 and 4, respectively), instead of ≥ 99% observed with **I** (Table 3, entry 6). Next, complex **IV**, analogue of complex **I** containing −Ph substituents instead of $-C_4H_6OMe$ on the cyclopentadienone ring, was also tested under the reaction conditions described above. Using **IV**/DBU ratios of 1/5000 and 1/10,000, formate was obtained in nearly quantitative yields (Table 3, entries 7 and 8). At lower ratio **IV**/DBU = 1/100,000, in a 72 h run, a TON value of 56,582 (Table 3, entry 9) was obtained. On the other hand, when complex **V**, i.e. the NHC-free dimeric precursor of **IV** was used, lower formate yields were observed both with and without the addition of TMANO (Table 3, entries 10 and 11), confirming that the presence of the NHC ligand has a greater impact on the catalytic performance compared to the type of substituents on the cyclopentadienone ring. Two iron analogue complexes **VI** and **VII** were tested under the reaction conditions applied for the Ru catalysts. Low formate yields were observed with these complexes (Table 3, entries 12–15), probably due to their lower thermal stability under the applied reaction conditions (100 °C, 24 h) compared to the Ru counterparts.

2.2. Mechanistic studies

In order to elucidate key aspects of the reaction mechanism such as the activation of pre-catalyst and the evolution of ruthenium species, ^{1}H NMR experiments on stoichiometric reactions involving **I** (named **1** from here onwards) were initially carried out. Complex **1** (10 mg) was dissolved in THF-d_8 (500 μL) and TMANO (100 equiv. to **1**) was added to the solution. The formation of trimethylamine (TMA) was observed at 2.13 ppm (Fig. S36), confirming that pre-catalyst activation occurs to give the putative complex [Ru(η^4-PhOMe$_2$Ph$_2$C$_4$CO)(CO)(NHC)(X)] (**2,** X = solvent, null). The CO released from the metal coordination sphere is converted to CO_2 by reaction with TMANO, that in turn is reduced to TMA. Next, another experiment was carried out to try to underpin the activation of dihydrogen by **1** with possible formation of [Ru(η^4-PhOMe$_2$Ph$_2$C$_4$CO)(CO)(NHC)(η^2-H$_2$)] (**2-H$_2$**) or [RuH(η^4-PhOMe$_2$Ph$_2$C$_4$CO)(CO)(NHC)]$^-$ (**3**). To a screw-cap NMR tube containing a solution of **1** (10 mg), TMANO (100 equiv.), DBU (100 equiv.) in THF-d_8 (500 μL), placed in an ice bath to avoid solvent evaporation, H_2 gas (1 bar) was bubbled through for 10 min. The tube was shaken and let to warm to room temperature, then heated to 60 °C for 15 min in an oil bath. After this time, the ^{1}H NMR spectrum (Fig. S37) showed a new singlet in the

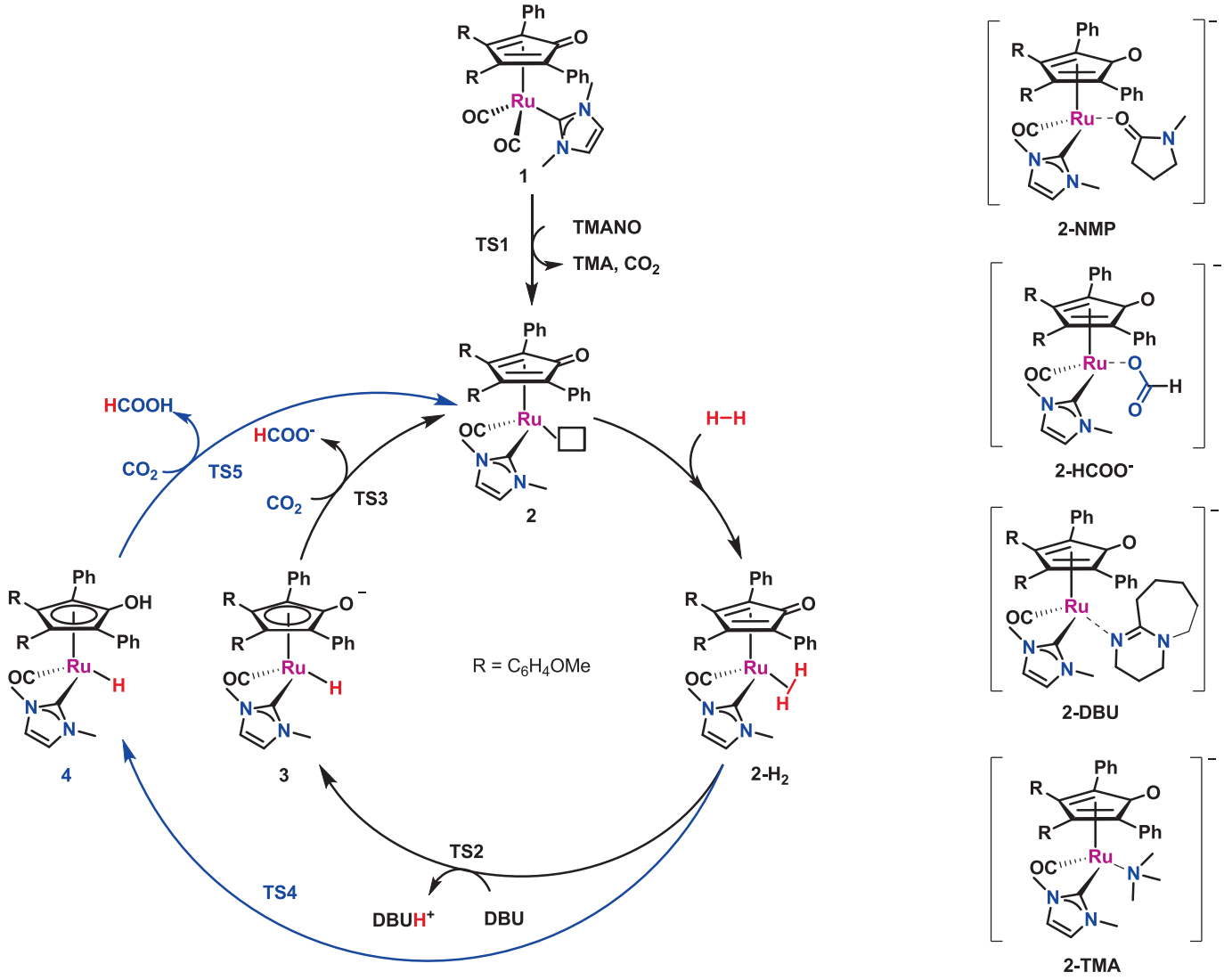

Scheme 2. Proposed catalytic mechanisms for CO_2 hydrogenation in the presence of **1**.

negative chemical shift range at −14.55 ppm, in the region typically expected for Ru-hydrido species. These NMR experiments confirm that pre-catalyst activation with TMANO is required to generate a coordination vacancy on Ru that is then readily available for heterolytic hydrogen splitting to give **3** in the presence of base. Attempts to independently synthesize and isolate complex **3** under various reaction conditions failed, due to the limited stability of this species in solution, hampering any workup.

Density functional theory (DFT) calculations were then carried out to gain further insights into the reaction and propose a catalytic mechanism (Scheme 2 and Supporting Information). DFT results confirmed that the activation of **1** occurs via a decarbonylative oxidation played by TMANO to give **2**. This step requires overcoming a free energy activation barrier (ΔG*) of 25.9 kcal/mol (**TS1**) and it is driven by an exergonic release of TMA and CO_2 (ΔG = -46.7 kcal/mol). The overall activation barrier comprises the endergonic formation of the adduct between **1** and **TMANO**, i.e. **1@TMANO**, which requires 10.7 kcal/mol, in line with experimental data (See Table 2). Since species **2** features a vacant coordination site on the ruthenium center, we computationally verified the thermodynamic stability of several **2**-ligand species, to evaluate the presence of stable complexes. Calculations showed that TMA (**2-TMA**, ΔG = -47.7 kcal/mol) and DBU (**2-DBU**, ΔG = -48.0 kcal/mol) stabilize the catalyst more than NMP (**2-NMP**, ΔG = -38.5 kcal/mol) or formate (**2-HCOO$^-$**, ΔG = -44.3 kcal/mol). Notably, **2** can also bind molecular hydrogen leading to **2-H_2**, with a ΔG = -39.5 kcal/mol, showing that H_2 coordination is thermodynamically competitive with other ligands binding. Then, two alternative pathways may follow for dihydrogen activation in **2-H_2**. The energetically preferred reductive pathway involves a DBU-assisted heterolytic cleavage of H_2 (black pathway in Scheme 2). This route proceeds via **TS2** (ΔG*= 8.5 kcal/mol) and yields the anionic intermediate **3** (ΔG = -45.0 kcal/mol), which exists in an acid-base equilibrium with its protonated form **4** (ΔG = -46.6 kcal/mol). Alternative to this pathway, a non-DBU-mediated dihydrogen splitting (**TS4**) might happen to form **4**, but this would require a much higher activation energy, i.e. ΔG*= 28.4 kcal/mol (blue pathway in Scheme 2). Next, the hydride complexes **3** and **4** can reduce CO_2 to either $HCOO^-$ or HCOOH, respectively. These reduction steps feature similar activation barriers, i.e. with ΔG* of 14.1 (**TS3**) and 15.1 (**TS5**) kcal/mol with **3** and **4**, respectively. The characterization of formate as thermodynamically favored product is in line with the experimental findings. Thus, considering the computed free energies surfaces of the catalytic cycles (Fig. 4), the CO_2 hydrogenation to formate catalyzed by **1** would preferentially occur via DBU-assisted heterolytic cleavage of molecular hydrogen. In summary, DFT calculations disclosed that the highest barrier in the mechanism is that related to the pre-activation of **1**, whereas rate-determining-step of the catalytic cycle is the insertion of CO_2 into the Ru-H bond. A key role is played by DBU in assisting the splitting of metal-coordinated molecular hydrogen.

3. Conclusions

In summary, the present study showed that phosphine-free ruthenium complexes supported by a strongly donating 1,3-dimethyl-imidazolyl ligand were able to bring about the efficient and selective hydrogenation of CO_2 to formate in the presence of a DBU as base and TMANO as co-catalyst, reaching TONs over 54,000 in single batch runs, at a catalyst loading as low as 0.001 mol%. Catalyst recycling experiments showed that the catalytic mixture containing **I** could be reused for up to 4 consecutive runs by simple re-pressurization, without significant losses in activity, giving an overall TON = 41,374. Control experiments showed that the presence of NHC has a more profound effect for catalysis than the variation of substituents on the cyclopentadienone ring. Finally, mechanistic experiments confirmed the proposed effect of TMANO in the pre-activation step. DFT calculations disclosed that the highest barrier of the entire process is the activation of the catalyst via the CO elimination by TMANO, and disclosed the pivotal role played by DBU in assisting the hydrogen splitting step.

4. Experimental Section

4.1. General procedure for carbon dioxide catalytic hydrogenation

In a typical experiment, the catalytic mixture containing solvent, catalyst, base and additive (if any) was prepared in a Schlenk tube under nitrogen. It was subsequently injected into a 40 mL magnetically stirred teflon-lined stainless steel autoclave built at CNR-ICCOM, kept under a

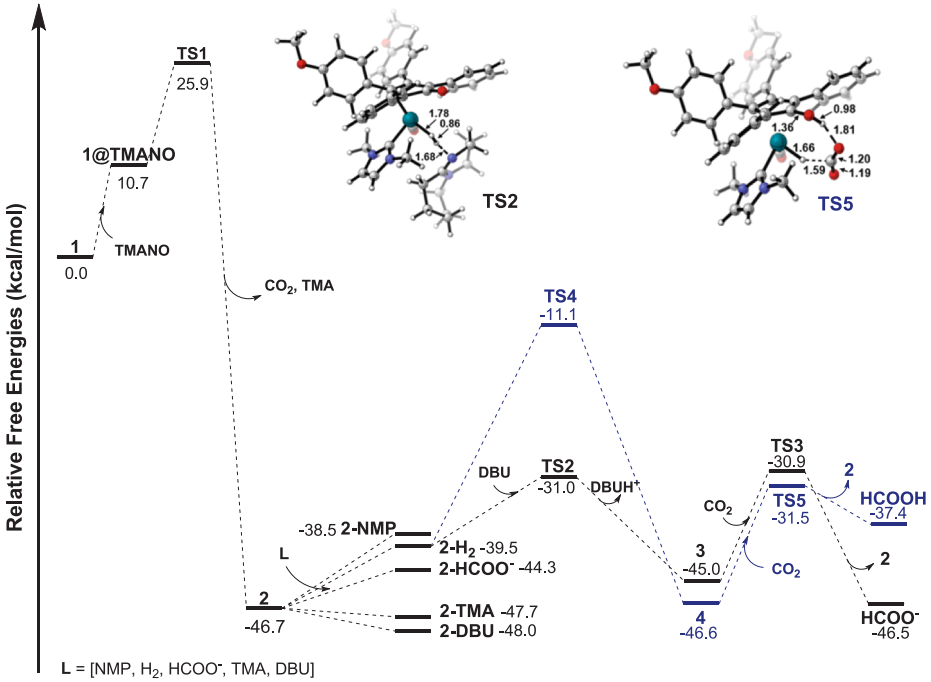

Fig. 4. Calculated free energy profile for CO_2 hydrogenation catalyzed by **1**.

nitrogen atmosphere. Then, the autoclave was pressurized with a H_2/CO_2 gas mixture at the desired pressure, placed into an oil bath pre-heated to the target temperature and stirred at 500 rpm for the set reaction time. After the run, the autoclave was cooled to below 10 °C using an ice bath. The pressure was gently released, and the reaction mixture was transferred into a round bottom flask. The autoclave beaker was thoroughly rinsed with H_2O and the washings were added to the rest of the mixture. The volume of the mixture was then gently reduced by using a rotary evaporator at room temperature until a homogeneous mixture was obtained. DMF (300 mL) was added to the mixture as internal standard and the formate content was determined by integrating the corresponding ^{1}H NMR signal vs. DMF. D_2O (ca. 0.7 mL) was added as deuterated solvent. All tests were repeated at least twice to ensure reproducibility (average error ca. 6%).

4.2. Synthesis of complex IV

Complex **IV** was synthesized by reacting 300 mg (1 equiv.) of complex **III** with 155 mg (2.4 equiv.) of silver oxide (Ag_2O) and 156 mg (2 equiv.) of 1,3-dimethylimidazolium iodide. The reaction was carried out in a 100 mL two-necked flask under an inert atmosphere (N_2), using 15 mL of dichloromethane as the solvent. The mixture was stirred at room temperature for 1 h and the reaction progress was monitored by FT-IR spectroscopy. The crude product was then filtered through a Gooch crucible with Celite to remove the byproduct (AgI). After concentration under vacuum, the resulting product was purified by column chromatography on alumina, using a dichloromethane/ethyl acetate mixture (100:0 to 0:100) as the eluent. Complex **IV** was obtained as a yellow solid obtained with a 56% yield. The complex is stable to air, moisture, in solution of organic solvents and in the presence of water. Characterization data: ^{1}H NMR (599.7 MHz, $CDCl_3$): δ 7.79 (m, 4H, CH_{aryl}), 7.17–7.04(m, 10H, CH_{aryl}), 6.76 (s, 2H, CHNHC), 6.65 (m, 4H, CH_{aryl}), 3.09 (s, 6H, $-NCH_3$). ^{13}C NMR (150.8 MHz, $CDCl_3$, g-HSQC, g-HMBC): δ 202.47 (CO), 172.72 ($C_{carbene}$), 169.33 (C=O, Cp), 135.43 (Cq_{aryl}), 133.62 (CH_{aryl}), 129.16 (CH_{aryl}), 127.43 (CH_{aryl}), 125.27 (Cq_{aryl}), 124.90 (CH_{aryl}), 123.62 (CHNHC), 112.93 (CH_{aryl}), 103.85 (C2,5, Cp), 78.46 (C3,4, Cp), 38.23 (–NCH_3). IR (CH_2Cl_2, cm^{-1}): 2005, 1946 (νCO); 1587 cm^{-1} (νC=O); ESI-MS (m/z) (+): 639 $[M + H]^+$; 662 $[M + Na]^+$. Anal. Calcd (%) for $C_{36}O_3N_2H_{28}Ru$: C, 67.81; H, 4.43 Found: C, 67.78; H, 4.38.

CRediT authorship contribution statement

Sylwia Kostera: Writing – original draft, Methodology, Investigation, Formal analysis, Data curation. **Chiara Lenzi:** Writing – original draft, Methodology, Investigation, Formal analysis, Data curation. **Saikat Pal:** Investigation, Data curation. **Francesco Calcagno:** Writing – original draft, Methodology, Conceptualization. **Ivan Rivalta:** Writing – original draft, Supervision. **Rita Mazzoni:** Writing – review & editing, Supervision, Methodology, Funding acquisition, Conceptualization. **Luca Gonsalvi:** Writing – review & editing, Supervision, Project administration, Methodology, Funding acquisition, Conceptualization.

Declaration of competing interest

The authors declare that they have no known competing financial interests or personal relationships that could have appeared to influence the work reported in this paper.

Acknowledgments

This research was funded by the European Union – NextGeneration EU from the Italian Ministry of Environment and Energy Security POR H2 AdP MMES/ENEA with involvement of CNR and RSE, PNRR - Mission 2, Component 2, Investment 3.5 “Ricerca e sviluppo sull’idrogeno”, CUP: B93C22000630006 and under the National Recovery and Resilience Plan (NRRP), Mission 4, Component 2, Investment 1.1, Call for tender No. 104 published on 2.2.2022 by the Italian Ministry of University and Research (MUR), funded by the European Union – NextGenerationEU – Project PRIN 20225N5T5B “ALCOVAL” – CUP B53D23015120006 - Grant Assignment Decree No. 1064 adopted on 18/07/2023 by the Italian Ministry of University and Research (MUR). Mr. Carlo Bartoli (CNR-ICCOM) is gratefully thanked for building and servicing the steel autoclaves used in this study.

Appendix A. Supplementary data

Supplementary data to this article can be found online at https://doi.org/10.1016/j.jcat.2026.116896.

Data availability

No data was used for the research described in the article.

References

[1] a) C.B. Peres, P.M.R. Resende, L.J.R. Nunes, L.C. de Morais, Advances in carbon capture and use (CCU) technologies: a comprehensive review and CO_2 mitigation potential analysis, Clean Technol. 4 (2022) 1193–1207, https://doi.org/10.3390/cleantechnol4040073;
b) J.-P. Innocent Niyonkuru, Advancements in carbon capture and utilization (CCU) technologies, Res. Output J. Eng. Sci. Res. 3 (2024) 17–22. ISSN: 1115–6155;
c) E.I. Koytsoumpa, C. Bergins, E. Kakaras, The CO_2 economy: Review of CO_2 capture and reuse technologies, J. Supercrit. Fluids 132 (2018) 3–16, https://doi.org/10.1016/j.supflu.2017.07.029;
d) C. Hepburn, E. Adlen, J. Beddington, E.A. Carter, S. Fuss, N. Mac Dowell, J. C. Minx, P. Smith, C.K. Williams, The technological and economic prospects for CO_2 utilization and removal, Nature 575 (2019) 87–97.

[2] a) S.C. Peter, Reduction of CO_2 to chemicals and fuels: a solution to global warming and energy crisis, ACS Energy Lett. 3 (2018) 1557–1561, https://doi.org/10.1021/acsenergylett.8b00878;
b) O. Emmanuel, T.C.E. Rozina, Advances in carbon dioxide capture and conversion technologies: industrial integration for sustainable chemical production, Next Sustainab. 6 (2025) 100108, https://doi.org/10.1016/j.nxsust.2025.100108;
c) L. Xu, Y. Xiu, F. Liu, Y. Liang, S. Wang, Research progress in conversion of CO_2 to valuable fuels, Molecules 25 (2020) 3653, https://doi.org/10.3390/molecules25163653.

[3] a) J. Yao, F. Cao, Y. Han, Y. Wang, L. Tan, J. Sun, G. Yang, L. Shi, C1 chemistry: the stories of research and applications from Toyama, Resour. Chem. Mater. 3 (2024) 62–92, https://doi.org/10.1016/j.recm.2023.08.004;
b) X. Jiang, X. Nie, X. Guo, C. Song, J.G. Chen, Recent advances in carbon dioxide hydrogenation to methanol via heterogeneous catalysis, Chem. Rev. 120 (2020) 7984–8034, https://doi.org/10.1021/acs.chemrev.9b00723;
c) W.-H. Wang, Y. Himeda, J.T. Muckerman, G.F. Manbeck, E. Fujita, CO_2 hydrogenation to formate and methanol as an alternative to photo- and electrochemical CO_2 reduction, Chem. Rev. 115 (2015) 12936–12973, https://doi.org/10.1021/acs.chemrev.5b00197;
d) S. Kushwaha, J. Parthiban, S.K. Singh, Recent developments in reversible CO_2 hydrogenation and formic acid dehydrogenation over molecular catalysts, ACS Omega 8 (2023) 38773–38793, https://doi.org/10.1021/acsomega.3c05286;
e) R. Sen, A. Goeppert, G.K.S. Prakash, Homogeneous hydrogenation of CO_2 and CO to methanol: the renaissance of low-temperature catalysis in the context of the methanol economy, Angew. Chem. Int. Ed. 61 (2022) e20220727, https://doi.org/10.1002/anie.202207278.
f) CO_2 Hydrogenation catalysis (Ed. Y. Himeda), 1st Edition March 2021, Wiley-VCH, Weinheim, Germany, ISBN: 978-3-527-34663-9, https://doi.org/10.1002/9783527824113.

[4] G.A. Filonenko, R. van Putten, E.N. Schulpen, E.J.M. Hensen, E.A. Pidko, Highly efficient reversible hydrogenation of carbon dioxide to formates using a ruthenium PNP-pincer catalyst, ChemCatChem 6 (2014) 1526–1530, https://doi.org/10.1002/cctc.201402119.

[5] R. Tanaka, M. Yamashita, K. Nozaki, Catalytic hydrogenation of carbon dioxide using Ir(III)−pincer complexes, J. Am. Chem. Soc. 131 (2009) 14168–14169, https://doi.org/10.1021/ja903574e.

[6] a) B.G. Schieweck, N.F. Westhues, J. Klankermayer, A highly active non-precious transition metal catalyst for the hydrogenation of carbon dioxide to formates, Chem. Sci. 10 (2019) 6519–6523, https://doi.org/10.1039/C8SC05230A;
b) Y. Zhang, A.D. MacIntosh, J.L. Wong, E.A. Bielinski, P.G. Williard, B. Q. Mercado, N. Hazari, W.H. Bernskoetter, Iron catalyzed CO_2 hydrogenation to formate enhanced by Lewis acid co-catalysts, Chem. Sci. 6 (2015) 4291–4299, https://doi.org/10.1039/C5SC01467K;
c) D. Wei, R. Sang, P. Sponholz, H. Junge, M. Beller, Reversible hydrogenation of carbon dioxide to formic acid using a Mn-Pincer complex in the presence of lysine, Nat. Energy 7 (2022) 438–447, https://doi.org/10.1038/s41560-022-01019-4].

[7] a) J. Klankermayer, S. Wesselbaum, K. Beydoun, W. Leitner, Selective catalytic synthesis using the combination of carbon dioxide and hydrogen: catalytic chess at the interface of energy and chemistry, Angew. Chem. Int. Ed. 55 (2016) 7296–7343, https://doi.org/10.1002/anie.201507458;
b) K. Sordakis, C. Tang, L.K. Vogt;, H. Junge, P.J. Dyson, M. Beller, G. Laurenczy, Homogeneous catalysis for sustainable hydrogen storage in formic acid and alcohols, Chem. Rev. 118 (2018) 372–433, https://doi.org/10.1021/acs.chemrev.7b00182;
c) S. Kostera, L. Gonsalvi, Manganese(I) catalyzed CO_2 reduction processes in homogenous phase, ChemCatChem 16 (2024) e202301391, https://doi.org/10.1002/cctc.202301391.

[8] N.A. Eberhardt, H. Guan, Reduction of CO_2 Mediated or Catalysed by Pincer Complexes. Chapter 4 in Pincer Compounds (Ed. D. Morales-Morales), Elsevier, 2018, 67-99, ISBN 9780128129319, https://doi.org/10.1016/B978-0-12-812931-9.00004-9.

[9] a) H.-J. Knölker, J. Heber, C.H. Mahler, Transition metal-diene complexes in organic synthesis, part 14.1 regioselective iron-mediated [2+2+1] cycloadditions of alkynes and carbon monoxide: synthesis of substituted cyclopentadienones, Synlett (1992) 1002–1004, https://doi.org/10.1055/s-1992-21563;
(b) H.-J. Knölker, J. Heber, Transition metal-diene complexes in organic synthesis, part 18.1 iron-mediated [2+2+1] cycloadditions of diynes and carbon monoxide: selective demetalation reactions, Synlett (1993) 924–926, https://doi.org/10.1055/s-1993-22654;
(c) H.-J. Knölker, E. Baum, J. Heber, Transition metal-diene complexes in organic synthesis, part 25.1 cycloadditions of annulated 2,5-bis(trimethylsilyl) cyclopentadienones, Tetrahedron Lett. 36 (1995) 7647–7650, https://doi.org/10.1016/0040-4039(95)01614-N;
(d) H.-J. Knölker, H. Goesmann, R. Klauss, A novel method for the demetalation of tricarbonyliron ± diene complexes by a photolytically induced ligand exchange reaction with acetonitrile, Angew. Chem. Int. Ed. 38 (1999) 702–705, https://doi.org/10.1002/(SICI)1521-3773(19990301)38:5<702::AID-ANIE702>3.0.CO;2-W;
e) H.-J. Knölker, E. Baum, H. Goesmann, R. Klauss, Demetalation of tricarbonyl (cyclopenta-dienone)iron complexes initiated by a ligand exchange reaction with NaOH – X-ray analysis of a complex with nearly square-planar coordinated sodium, Angew. Chem. Int. Ed. 38 (1999) 2064–2066, https://doi.org/10.1002/(SICI)1521-3773(19990712)38:13/14<2064::AID-ANIE2064>3.0.CO;2-W.

[10] F. Zhu, L. Zhu-Ge, G. Yang, S. Zhou, Iron-catalyzed hydrogenation of bicarbonates and carbon dioxide to formates, ChemSusChem 8 (2015) 609–612, https://doi.org/10.1002/cssc.201403234.

[11] S. Coufourier, Q.G. Gaillard, J.-F. Lohier, A. Poater, S. Gaillard, J.-L. Renaud, Hydrogenation of CO_2 hydrogenocarbonate, and carbonate to formate in water using phosphine free bifunctional iron complexes, ACS Catal. 10 (2020) 2108–2116, https://doi.org/10.1021/acscatal.9b04340.

[12] Q. Chen, C. Shen, G. Zhu, X. Zhang, C.-L. Lv, B. Zeng, S. Wang, J. Li, W. Fan, L. He, Selectivity switching of CO_2 hydrogenation from HCOOH to CO with an in situ formed Ru−Li complex, ACS Catal. 11 (2021) 9390–9396, https://doi.org/10.1021/acscatal.1c01874.

[13] a) Y. Blum, D. Czarkie, Y. Rahamim, Y. Shvo, (Cyclopentadienone)ruthenium carbonyl complexes - a new class of homogeneous hydrogenation catalysts, Organometallics 4 (1985) 1459–1461, https://doi.org/10.1021/om00127a027;
b) Y. Shvo, D. Czarkie, Y. Rahamim, D.F. Chodosh, A new group of ruthenium complexes: structure and catalysis, J. Am. Chem. Soc. 108 (1986) 7400–7402, https://doi.org/10.1021/ja00283a041;
c) B.L. Conley, M.K. Pennington-Boggio, E. Boz, T.J. Williams, Discovery, applications, and catalytic mechanisms of Shvo's catalyst, Chem. Rev. 110 (2010) 2294–2312, https://doi.org/10.1021/cr9003133.

[14] a) E. Peris, Smart *N*-heterocyclic carbene ligands in catalysis, Chem. Rev. 118 (2018) 9988–10031, https://doi.org/10.1021/acs.chemrev.6b00695;
b) M.N. Hopkinson, C. Richter, M. Schedler, F. Glorius, An overview of N-heterocyclic carbenes, Nature 510 (2014) 485–496, https://doi.org/10.1038/nature13384.

[15] S. Sanz, A. Azua, E. Peris, '(η^6-arene)Ru(bis-NHC)' complexes for the reduction of CO_2 to formate with hydrogen and by transfer hydrogenation with ^{i}PrOH, Dalton Trans. 39 (2010) 6339–6343, https://doi.org/10.1039/C003220D.

[16] C. Cesari, S. Conti, S. Zacchini, V. Zanotti, M.C. Cassani, R. Mazzoni, Sterically driven synthesis of ruthenium and ruthenium–silver N-heterocyclic carbene complexes, Dalton Trans. 43 (2014) 17240–17243, https://doi.org/10.1039/C4DT02747G.

[17] a) C. Cesari, R. Mazzoni, E. Matteucci, A. Baschieri, L. Sambri, M. Mella, A. Tagliabue, F.L. Basile, C. Lucarelli, Hydrogen transfer activation via stabilization of coordinatively vacant sites: tuning long-range p-system electronic interaction between Ru(0) and NHC Pendants, Organometallics 38 (2019) 1041–1051, https://doi.org/10.1021/acs.organomet.8b00850;
b) C. Cesari, A. Cingolani, C. Parise, S. Zacchini, V. Zanotti, M.C. Cassani, R. Mazzoni, Ruthenium hydroxycyclopentadienyl N-heterocyclic carbene complexes as transfer hydrogenation catalysts, RSC Adv. 5 (2015) 94707–94718, https://doi.org/10.1039/C5RA18345F;
c) F. Calcagno, C. Cesari, A. Gagliardi, A. Messori, A. Piazzi, F. Tamassia, M. Garavelli, F. Himo, R. Mazzoni, I. Rivalta, Combined computational-experimental study of Ru(0)-catalyzed Guerbet reaction, Cell Rep. Phys. Sci. 5 (2024) 102291, https://doi.org/10.1016/j.xcrp.2024.102291.

[18] Y. Blum, Y. Shvo, Catalytically reactive ruthenium intermediates in the homogeneous oxidation of alcohols to esters, Israel J. Chem. 24 (1984) 144–148, https://doi.org/10.1002/ijch.198400024.

[19] A. Cingolani, C. Cesari, S. Zacchini, V. Zanotti, M.C. Cassani, R. Mazzoni, Straightforward synthesis of iron cyclopentadienone *N*-heterocyclic carbene complexes, Dalton Trans. 44 (2015) 19063–19067, https://doi.org/10.1039/C5DT03071D.

[20] S. Kostera, A. Gobbo, M. Guelfi, S. Zacchini, G. Manca, F. Marchetti, L. Gonsalvi, Carbon dioxide hydrogenation to formate catalyzed by highly active Ru-tris (pyrazolyl)methane complexes, J. Catal. 450 (2025) 116231, https://doi.org/10.1016/j.jcat.2025.116231.

[21] a) T.-Y. Luh, Trimethylamine *N*-oxide-a versatile reagent for organometallic chemistry, Coord. Chem. Rev. 60 (1984) 255–276, https://doi.org/10.1016/0010-8545(84)85067-5;
b) A.J. Pearson, Y. Yamamoto, Trimethylamine N-Oxide, Encyclopedia of Reagents for Organic Synthesis (2010), https://doi.org/10.1002/047084289X.rt268.pub2;
c) H.-J. Knölker, Trimethylamine *N*-Oxide-A Useful Oxidizing Reagent, J. Prakt. Chem. 338 (1996) 190–192, https://doi.org/10.1002/prac.19963380138.

[22] a) A. Inoue, H. Shinokubo, K. Oshima, Oxidative heck-type reaction involving cleavage of a carbon−phosphorus bond of arylphosphonic acids, J. Am. Chem. Soc. 125 (2003) 1484–1485, https://doi.org/10.1021/ja026758v;
b) C.A.M.R. van Slagmaat, K.C. Chou, L. Morick, D. Hadavi, B. Blom, S.M.A. De Wildeman, Synthesis and catalytic application of Knölker-type iron complexes with a novel asymmetric cyclopentadienone ligand design, Catalysts 9 (2019) 790, https://doi.org/10.3390/catal9100790;
c) A. Guðmundsson, J.-E. Bäckvall, On the use of iron in organic chemistry, Molecules 25 (2020) 1349, https://doi.org/10.3390/molecules25061349;
d) L. Pignataro, C. Gennari, Recent catalytic applications of (cyclopentadienone) iron complexes, Eur. J. Org. Chem. (2020) 3192–3205, https://doi.org/10.1002/ejoc.201901925;
e) B.K. Werley, X. Hou, E.P. Bertonazzi, A. Chianese, T.W. Funk, Substituent effects and mechanistic insights on the catalytic activities of (tetraarylcyclopentadienone)iron carbonyl compounds in transfer hydrogenations and dehydrogenations, Organometallics 42 (2023) 3053–3065, https://doi.org/10.1021/acs.organomet.3c00284.